Theoretical Study on the Decomposition of N_2O over Alkaline Earth Metal-Oxides: MgO−BaO

Elly J. Karlsen,[†] Martin A. Nygren,[‡] and Lars G. M. Pettersson*[,‡]

Oil and Energy Research Centre Porsgrunn, Section for Hydrocarbon Processes and Catalysis, Norsk Hydro ASA, N-3907 Porsgrunn, Norway and FYSIKUM, SCFAB, Stockholm University, S-106 91 Stockholm, Sweden

Received: February 11, 2002; In Final Form: May 25, 2002

The decomposition of N_2O through oxygen abstraction and surface peroxide ion formation is studied over the whole sequence, MgO−BaO, of alkaline-earth rock-salt metal oxides. The initial barrier to abstraction follows the expectations (MgO > CaO > SrO > BaO) of O^{2-} chemistry. Good agreement with experiment is obtained for MgO and CaO, but for BaO the discrepancy is large. Consideration of both the Langmuir−Hinshelwood and the Elay−Rideal mechanisms suggests that for MgO the surface is regenerated already at low peroxide ion coverage through diffusion and recombination. For CaO, diffusion is hindered and recombination probably occurs only at higher peroxide ion coverage obtained through deposition of oxygen. SrO and BaO allow neither diffusion over the surface nor recombination of oxygen from two surface peroxide ions. Instead, the Elay−Rideal mechanism becomes active with activation energy at high coverage in good agreement with the experiment for BaO.

1. Introduction

Nitrous oxide (N_2O) is produced as a byproduct from several industrial processes, and some examples are the oxidation of ammonia to yield nitric acid in the production of fertilizers and from adipic acid in the production of nylon. From an environmental viewpoint, the continued outlet of N_2O in the atmosphere constitutes a severe problem since it contributes to the catalytic destruction of stratospheric ozone and furthermore is a powerful greenhouse gas (corresponding to 310 CO_2 equivalents). This was, for instance, recognized in the Kyoto Protocol on Climate change from 1997 and has led to an increased focus on reducing the outlet of man-made nitrous oxide. In Europe, nitrous oxide constitutes 9% of the total greenhouse gas emission, and the main sources are agriculture, passenger-car catalysts, and industrial processes such as nitric and adipic acid production.[1] Reduction of the outlet of N_2O from stationary plants can be achieved through catalytic decomposition in the off-gas. Since the temperature in the off-gas is relatively low (230−250 °C), the catalysts must be active at low temperature to avoid an economically costly postreaction heating of the off-gases for the conversion. So far, the required low-temperature running catalysts have, however, not been identified. Two classes of compounds presently seem to hold the greatest promise: zeolites and the alkaline-earth oxides, in particular we find in the present work that BaO should have a very low barrier to the initial abstraction of oxygen from N_2O. Here, we will focus on the properties of the alkaline-earth oxides and discuss the factors determining the specific reactivity. The temperatures required for the conversion, as deduced from experiment, are in the appropriate range with activity toward N_2O decomposition at relatively low temperatures (230−600 °C).[2] The most well-studied systems are the MgO and CaO substrates for which the catalytic activity has been studied by several authors. Nakamura et al.[3] observed large amounts of molecular oxygen desorbing after exposure to N_2O but not after exposure to O_2. They proposed that surface peroxide ions (O_2^{2-}) are involved in the mechanism of the N_2O decomposition reaction[4,5] and suggested the following steps in an overall catalytic cycle involving as the second step the regeneration of the active site:

$$N_2O + O^{2-}{}_{(surf)} \rightarrow N_2 + O^{2-}{}_{2(surf)} \quad (1)$$

$$O^{2-}{}_{2(surf)} + O^{2-}{}_{2(surf)} \rightarrow O_2 + 2O^{2-}{}_{(surf)} \quad (2)$$

Step 1 follows the so-called Elay−Rideal (ER) mechanism, where N_2O is dissociatively adsorbed followed by release of N_2. This step is generally envisaged as charge donation from the catalyst into the antibonding orbitals of N_2O. In addition to metal oxides, metal surfaces as well as F-centers and coordinatively unsaturated sites in transition-metal-exchanged zeolites can act as such centers.[6−8] The surface is regenerated in step 2 via the Langmuir−Hinshelwood (LH) mechanism where one has a recombination of the adsorbed oxygens. This regeneration step has been considered in previous work on alkaline-earth oxides.[9] However, as we will show in the present work, the critical parameter in the O_2 desorption through recombination is the lattice parameter and thereby the O−O distance, which limits the efficiency of this process for several of the substrates. An alternative route has thus also been considered in the present work. Here, the regeneration of the active site is by oxygen removal via the ER mechanism:

$$N_2O + O^{2-}{}_{2(surf)} \rightarrow N_2 + O_{2(gas)} + O^{2-}{}_{(surf)} \quad (3)$$

The ER mechanism for regeneration of the active sites has, for instance, been considered for transition-metal-exchanged ZSM-5 zeolites.[10,11] As this catalytic cycle indicates, for a particular material to perform well as a catalyst, there should be a balance between the activation barrier for the decomposition reaction and the stability of the formed surface peroxide ion, which determines the barrier to regenerate the surface. That is, the

* To whom correspondence should be addressed. E-mail: lgm@physto.se.
[†] Oil and Energy Research Centre Porsgrunn.
[‡] Stockholm University.

10.1021/jp025622g CCC: $22.00
Published on Web 07/31/2002

activation barrier should be as low as possible, while the stability of the formed peroxide ion should not be too high. All the reaction steps (1−3) given here will be considered in the present work. The fundamental idea of the present work is based on the factors determining the reactivity of the anions leading to what can be called an O^{2-} chemistry. The idea has been proposed in earlier works by Pettersson and co-workers[5,12] and by Pacchioni et al.[4] and applied to a discussion of N_2O decomposition over MgO and CaO by Snis and Miettinen.[13] More recently, Idriss et al.[14] have discussed the importance of the lattice potential in a general sense in metal-oxide chemistry. The fundamental observation is that O^{2-} is unstable in a vacuum and can only exist if stabilized by an external potential, such as the Madelung potential in a metal-oxide crystal. For an oxide with a small lattice parameter, the Madelung potential is strong, leading to a stabilization of the anion and to a resulting closed-shell, neon-like behavior. This is the case, for example, for MgO. If one imagines a hypothetical expansion of the lattice out to infinity, there will be some point at which the potential is too weak to stabilize the extra charge and one electron must be transferred to the cation. In the group of the alkaline-earth metals, we find a sequence of rapidly increasing lattice parameters for their oxides (MgO 4.21 Å, CaO 4.81 Å, SrO 5.16 Å, and BaO 5.52 Å[15]), and we can expect a parallel increase in the electron-donating properties of the anions as the stabilization is reduced with the increasing lattice parameters. This should lead to an enhancement of the stability of the peroxide ions that have been proposed to be formed from the decomposition of N_2O over these oxides, and, as a consequence, also to a reduction of the barriers to the elementary abstraction step. The latter follows simply from the fact that the reactants (N_2O and metal oxide) are the same in each case, the reaction mechanism is the same for each system, but the stability of the products (surface peroxide ions and N_2) is stepwise enhanced in the sequence from MgO to BaO. Viewing the barrier as the result of an avoided crossing between the reactant and product states, the enhanced product stability leads to an earlier crossing and thus to a lower barrier. The enhanced stability of the formed surface peroxide ions has also been reported for MgO and CaO in the work by Nygren and Pettersson.[5] This trend was also found in the combined experimental and theoretical work by Snis and Miettinen,[13] where CaO showed higher activity toward N_2O decomposition compared to that for MgO. Thus, having this in mind, one would expect an enhanced activity toward N_2O decomposition when following the sequence MgO, CaO, SrO, and BaO. Starting from MgO and CaO, where the experimentally estimated activation energies for N_2O decomposition are, respectively, 36 and 26 kcal/mol,[13] one would expect even lower activation energies for SrO and BaO. In a recent experimental work by Xie and Lunsford,[16] the obtained result for N_2O decomposition on BaO is, however, in contradiction with this trend with an activation energy estimated to be 33 kcal/mol, which is very similar to that of MgO (36 kcal/mol). The experiment was performed using BaO supported on MgO (Ba/MgO), and the system was active for the steady-state decomposition reaction above 600 °C. The reaction was first-order with respect to the concentration of N_2O, and peroxide ions were observed as decomposition products. In contrast to what has been found for the reaction over MgO and CaO, the reaction was inhibited by the presence of O_2. Also in this case, surface peroxide ions were formed, which suggests that peroxide ions can be formed through the reverse of reaction 2. Indeed, it is well known that BaO and BaO_2 are in equilibrium with a composition that depends on the partial pressure of oxygen over the oxide.

2. Computational Details

It is well known that the highest reactivity on a metal-oxide substrate typically is associated with low-coordinated sites (steps, corners, kinks, etc.) and various defects at the surface. In the present work, we have still chosen to consider only the five-coordinated regular terrace sites of the respective (100) faces of the crystals, but we will obtain general trends through a comparison along the MgO to BaO sequence. The computed binding energies can be expected to provide lower bounds for the maximum obtainable on any site of the surface and, correspondingly, the computed barriers should give upper bounds for the reactions at lower-coordinated sites. However, in earlier work good agreement for measured and computed barriers has been found for the reaction at the five-coordinated terrace sites of MgO(100) and CaO(100).[13] The surface is represented by embedded cluster models, where we have employed a Me_5O_5 (Me = Mg, Ca, Sr, or Ba) cluster for the adsorption study. For the studies of the regeneration of the surface through the LH and ER mechanisms, larger models were used: $Me_{16}O_{16}$ and Me_9O_9 for LH and ER, respectively. More detailed discussions of the models employed are given in the respective sections. To represent the lattice outside the cluster, the ab initio Model Potential (AIMP)[17,18] embedding approach has been used together with an explicit representation of the full Madelung potential of the different lattices. The AIMP embedding approach has proven to be successful in representing the lattice effects on cluster properties in several studies involving ionic crystals.[17,24,25] This approach provides an approximate description of the short-range Coulomb (incomplete screening), exchange, and orthogonality interactions, as well as a representation of relativistic effects, on the basis of the frozen ions.[17,18] The nuclear attraction integrals over the Madelung potential were computed through the proper Ewald summation using the approach of Parry.[19,20] These integrals and the AIMP (core and embedding) potential integrals have been implemented in the ECPAIMP program[21] and have recently been interfaced to the Gaussian94/98 package by Nygren and Hall.[22,23] Ions out to a distance of 11.3 Bohr from any cluster ion are here represented by AIMP, and the parameters have been taken from.[24,25] All geometries and energies were obtained at the B3LYP level. Transition-state geometries were determined by employing energy and gradient calculations along the reaction path. The central oxygen in the adsorption studies and the central Me_4O_4 unit for the oxygen recombination study were allowed to relax while the remaining cluster ions were kept fixed. This approach was tested for MgO, where also unembedded MgO cluster models can be used[26] and the full Hessian computed.

The Huzinaga MIDI-4 basis[27] was used for the magnesium cation. For Ca, Sr, and Ba, the core electrons were described by effective core potentials (ECP) and only the outermost valence electrons were explicitly treated in the calculations. Both the core potential and the valence basis set were taken to be those of Hay and Wadt.[28] Oxygen and nitrogen were described by the Dunning double-ζ basis set[29] extended with a diffuse p and a d function for polarization. For the lattice anions, an additional diffuse s-function was added and all the diffuse functions were optimized for the cluster.[24]

3. Results and Discussion

The results from the present work are divided in three parts. We will first present results on the formation of peroxide ions

TABLE 1: Binding Energies (in kcal/mol) and Geometries (Å) for Surface Peroxide Ions[a]

	$O + Me_5O_5 \rightarrow O_2Me_5O_4$		
substrate	$r(O^{2-}\cdot\cdot O_{ads})$	$\Delta z(O^{2-})$	ΔE (kcal/mol)
MgO	1.55	−0.11	34.6
CaO	1.53	−0.18	61.8
SrO	1.53	−0.25	73.1
BaO	1.53	−0.27	81.4

[a] $\Delta z(O^{2-})$ denotes the vertical displacement of the central surface oxygen.

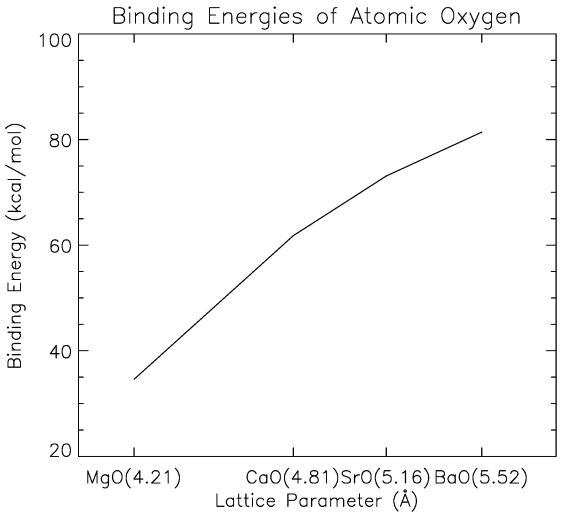

Figure 1. Binding energy (in kcal/mol) of atomic oxygen on MgO, CaO, SrO, and BaO.

on the whole sequence from MgO to BaO. In the second and third parts, we will focus on the activation of N_2O giving N_2 and O_2^{2-} on these oxides and the subsequent regeneration of the oxide surface. These parts are also devoted to a discussion of the findings in the present work and in particular in the light of previous experimental work.

3.1 Formation of Surface Peroxide Ions. The geometries and binding energies (relative to ^3P atomic oxygen) of the formed surface peroxide ions are given in Table 1, where it is immediately seen that the reaction energy for the formation of the surface peroxide ions increases monotonically when following the sequence MgO to BaO. The reactivity is related to the ability of the surface oxygen anion to donate electrons to the adsorbate, which again is related to the stabilization of the surface oxygen anion. At the oxygen sites, the Madelung potential is positive and stabilizes the doubly charged oxygen anions. The electrostatic potential decreases with increasing lattice parameter and as a consequence the reactivity of the anions increases in the sequence MgO to BaO. This trend is displayed in Figure 1, where one can clearly see a correlation between binding energies and the lattice parameter of these oxides.

Another aspect of the larger lattice parameter is that the volume or cavities in which the anions reside become larger. As a result, the oxygen anion in BaO can relax more into the bulk compared to the case for MgO. As can be seen in Table 1, the O_2^{2-} movement into the bulk is less pronounced for MgO compared to the other oxides. This relaxation enhances the stabilization of the resulting peroxide ions by allowing sharing of charge between the two oxygens while keeping the center of charge within the surface.

For MgO, there have been some discrepancies in the literature regarding the binding energy in the surface peroxide ion. Nygren and Pettersson[5] obtained a low value of 10.4 kcal/mol for a minimal model consisting of an O^{2-} anion embedded using projection operators and concluded that the activity of MgO should be associated with defects. Kantorovich et al. obtained a substantially higher value of 46 kcal/mol in slab model DFT calculations.[30] This was later challenged by Xu and co-workers, who obtained 25.3 and 19.6 kcal/mol at the B3LYP and MP2 levels, respectively.[31] Embedded Mg_5O_5 clusters were used and, similar to Kantorovich and Gillan, they obtained a minimum energy for a geometry where the peroxide ions tilt toward the neighboring anion. In the present work, we find a similar geometry for the peroxide ion. The present value of 34.6 kcal/mol for the embedded Mg_5O_5 cluster is intermediate between the two recent values but would still predict an endothermic reaction for the N_2O decomposition compared to the $N_2O \rightarrow N_2 + O$ reaction energy of about 40 kcal/mol.[32] To establish the reliability of this prediction and furthermore to investigate the accuracy of the embedding procedure for internal peroxide binding energies, we have tested the convergence with the size of the cluster. Here, we applied Mg_5O_5 embedded as the smallest model and increased further to Mg_9O_9 gas-phase cluster (the smallest that can be used), to Mg_9O_9 embedded cluster, and finally to $Mg_{25}O_{25}$ gas-phase cluster. The binding energies converge nicely from 34.6 kcal/mol for the smallest model, to 38.3 kcal/mol for the Mg_9O_9 cluster, 37.8 kcal/mol for the embedded Mg_9O_9 model, and finally, 37.3 kcal/mol for the large $Mg_{25}O_{25}$ gas-phase cluster. Thus, we conclude that the N_2O decomposition will be close to thermoneutral on MgO and that the embedding procedure gives results that are reliable to within about a couple of kcal/mol. For MgO, it is appropriate to use either embedded or gas-phase clusters (cf. results for Mg_9O_9), and the effect of the embedding is only to allow a somewhat smaller cluster to be used. For SrO and BaO, the stabilizing potential is too weak for employing an unembedded Me_9O_9 cluster; substantially larger and computationally unwieldy clusters must be used to establish the appropriate charge distribution. In this case, the use of the embedding is of critical importance.

3.2 Activation Barrier for the N_2O Decomposition Reaction. The N_2O decomposition reaction over rock-salt metal oxides has been reviewed by Kapteijn et al.[2] and the proposed catalytic cycle deduced both from experiment and theory includes steps 1 and 2 as indicated in the Introduction. The rate of the overall reaction is most likely proportional to the partial pressure of N_2O.[2] Snis and Miettinen[13] conclude that the rate at steady state is determined by the oxygen abstraction from N_2O at low N_2O concentration and possibly by oxygen desorption at high N_2O concentration. The reactions over MgO and CaO seem not to be affected by the presence of molecular oxygen and, indeed, several experimental works on MgO and CaO show no subsequent desorption of O_2 from the surface after exposure to molecular oxygen. This is not the case for BaO. Here, peroxide ions were observed and were suggested by Xie and Lunsford[16] to be formed by the reverse of reaction 2.

The trend of the calculated binding energies for surface peroxide ions suggests that the activation barrier for N_2O decomposition should decrease in the sequence MgO, CaO, SrO, and BaO. This trend was found for MgO and CaO in the experimental and theoretical study by Snis and Miettinen.[13] They calculated activation barriers of 36.4 and 24.4 kcal/mol for MgO and CaO, respectively, which is in agreement with our results. As the results in Table 2 and Figure 3 show, this trend is found to hold for the whole sequence, that is, the activation barrier

TABLE 2: Transition-State Structure (Å) and Activation Barriers (kcal/mol) for the Oxygen Abstraction Step in the Decomposition of N_2O[a]

substrate	r(N−N)	r(N−O)	r(O−O^{2-})	Δz(O^{2-})	$\Delta E^{\#}$ (kcal/mol)
MgO	1.12	1.64	1.92	0.01	37.1
CaO	1.13	1.53	2.04	−0.02	24.6
SrO	1.13	1.49	2.09	−0.05	19.7
BaO	1.13	1.47	2.12	−0.10	16.0

[a] Δz(O^{2-}) describes the displacement of the central surface oxygen relative to the (001) surface.

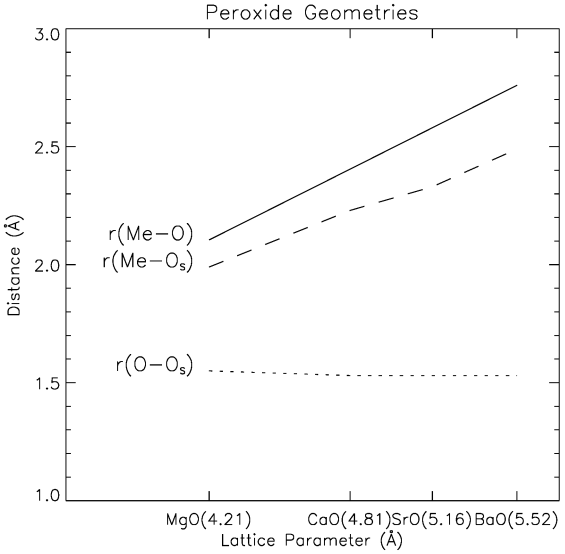

Figure 2. Peroxide ion geometry for MgO, CaO, SrO, and BaO. r(Me−O) is the crystal metal−oxygen bond distance. r(Me−Os) denotes the bond distance of the central surface oxygen anion and the bulk metal cation. r(O−Os) is the bond distance in (O_2^{2-}).

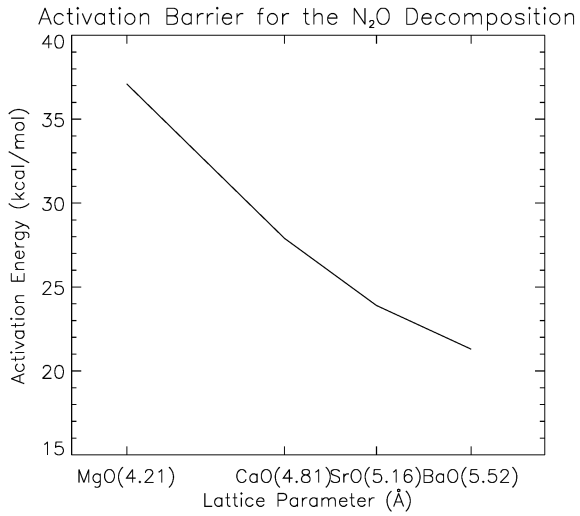

Figure 3. Activation energy (kcal/mol) for the N_2O oxygen abstraction step.

for this decomposition reaction follows the sequence MgO > CaO > SrO > BaO. BaO shows the lowest computed activation barrier (16 kcal/mol), which is about half of that for MgO in strong contradiction to the experimentally determined activation barrier of 33 kcal/mol by Xie and Lunsford.[16] The surface basicity or ability of lattice O^{2-} to donate electrons has been shown to correlate well with the catalytic activity (see ref 33 and references therein). As a result of the increasing interaction, the N−O bond distance in the transition state becomes shorter when going from MgO to BaO (see Figure 4). The more

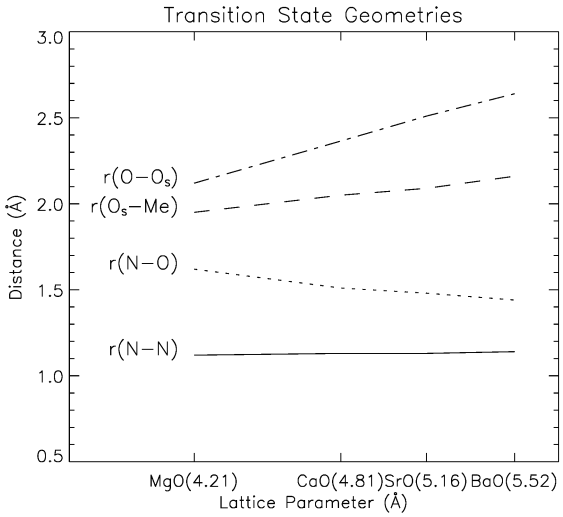

Figure 4. Geometry of transition-state structures for MgO, CaO, SrO, and BaO. r(O−Os) denotes the $N_2O-O_{surface}$ bond distance, r(Os−Me) the bond distance of the central surface oxygen and bulk metal, r(N−O) is the NN−O bond distance, and r(N−N) the N−NO bond distance in N_2O.

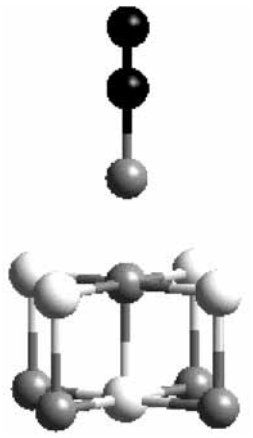

Figure 5. Transition-state structures for the oxygen abstraction step in the N_2O decomposition reaction over alkaline-earth oxide. Oxygen is colored gray, nitrogen black, and metal white.

stretched N−O distance for MgO is reflected in the highest barrier for this case; conversely, the shortest distance and lowest barrier are found for BaO. The relationship between transition-state geometry and barrier was also pointed out in the work by Snis and Miettienen for MgO and CaO.[13] This can also be noted in the increased distance of N_2O to the surface at the transition state. Again, the movement of the central oxygen into the bulk is more pronounced for BaO than for MgO, which serves to stabilize the resulting peroxide ions. The transition-state structure is displayed in Figure 5 and was obtained by stepwise optimization using the $O_{surface}-O_{NNO}$ as the reaction coordinate. The remaining parameters (O−N, N−N, and Ba−$O_{surface}$ distances) were optimized at each step with N_2O restricted to be linear. The structure was checked by also performing the calculations for the unembedded Mg_9O_9 cluster for which second derivatives and frequencies can be computed to identify the TS. The geometry at the TS is quite similar to the one obtained using the Mg_5O_5 embedded model (see Table 2). The optimized r(N−N) distance is 1.12 Å, the r(N−O) distance is 1.63 Å, and finally, the r(O−O^{2-}) bond distance is calculated to 1.92 Å. The distance of the central surface anion relative to the (100) surface (Δz(O^{2-})) is here −0.02 Å. The barrier is also similar and is calculated to 37.6 kcal/mol. The vibration frequencies at

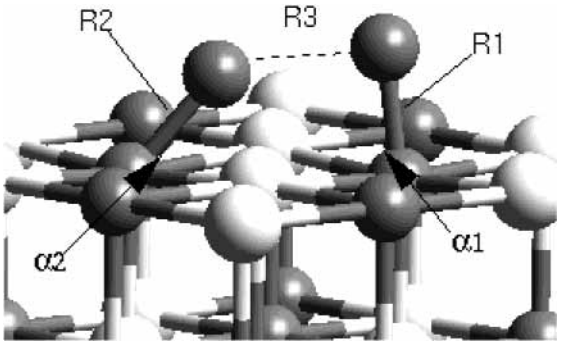

Figure 6. Transition-state structures of O_2 desorption from MgO and CaO. The oxygen is given in gray and metal in white. See Table 3 for the corresponding geometry data. Oxygen is given in gray and metal in white.

the transition state show two imaginary modes, and the one at -650 cm^{-1} corresponds to the mode that transfers the N_2O to N_2 and adsorbed oxygen. The second and the third imaginary modes (85.0 cm^{-1}) are due to the constraint to linearity during the optimization. The low value of these two modes indicates, however, that the energy surface for an angular movement of the linearly adsorbed N_2O is rather shallow. The good agreement between the bare cluster and embedded model suggests that the calculations using the Me_5O_5 embedded models give a qualitatively good picture of the transition state and the activation barrier, in particular in the comparison of the different oxides.

All in all, the computed barriers to surface-assisted abstraction of oxygen from N_2O are thus found to conform to what would be expected from the simple considerations of the O^{2-} chemistry. The stability of the produced peroxide ions, and as a consequence the barrier heights, are direct results of the lattice parameters. The reaction that has been considered so far leads to a peroxide ions covered substrate and gas-phase N_2. To understand the sustained catalytic activities, we must now also consider the regeneration of the surface to complete the catalytic cycle.

3.3 Regeneration of the Surface. We will here consider two possible reaction routes to regenerate the substrate. The first will follow the Langmuir−Hinshelwood (LH) mechanism where one has a direct recombination of two surface peroxide ions to form gas-phase O_2 (reaction step 2). The second follows the Elay−Rideal (ER) mechanism with a direct reaction between surface peroxide ions and gas-phase N_2O and is given in reaction 3.

Both mechanisms can be expected to be strongly dependent on the lattice parameter through the distance between anions in the former case, affecting both the surface diffusion and recombination of oxygen and the stability of the peroxide ions at the surface in the latter case. Calculated barriers thus indicate that oxygen surface diffusion will begin at increasingly higher temperatures for the series MgO < CaO < SrO and will not occur on BaO as competing processes become dominant at a lower temperature. This is due to the long oxygen−oxygen distance in the BaO surface, which forces the adsorbed oxygen atom to completely break the bond to the first oxygen anion before a new bond can start to develop.

The Langmuir−Hinshelwood Mechanism. Beginning with the direct recombination of two peroxide ions, this process has been considered for MgO and CaO by Snis and Panas.[9] The pathway to recombination that was considered in their work and in the present case is illustrated in Figure 6. The surface-bound peroxides are each in the singlet state, which implies that after recombination the O_2 molecule will be found in the $^1\Delta_g$ excited state. The lowest barrier was found to occur for an asymmetrical configuration where the internal peroxide ion bond is broken only for one of the involved oxygens. This is also found in the present work where the model has been extended to a $Me_{16}O_{16}$ gas-phase cluster for MgO and CaO. This model is sufficient for describing the recombination barrier on MgO and CaO, since these systems, in addition to the size of the model used here, are more strongly stabilized by the local charges than oxides, such as SrO and BaO, with larger lattice parameter. For the unembedded clusters, we can apply second derivatives and thereby obtain the TS including vibration frequency analysis. Since the gas-phase clusters used here are large, we expect that the TS geometry and activation barrier will not change much upon using embedded models, even for CaO. Single-point energy calculations for embedded $Me_{16}O_{16}$ clusters give the same activation barrier for MgO (19.6 kcal/mol), while for CaO, the activation barrier (39.3 kcal/mol) for the embedded model is only 1.2 kcal/mol higher than that obtained using the gas-phase $Me_{16}O_{16}$ cluster model. The vibration frequency analysis for the TS geometry for both MgO and CaO shows only one imaginary frequency mode (452 and 448 cm^{-1}, respectively). This vibration frequency corresponds to the mode that transfers one of the peroxide ions to the other leading to the formation of O_2. For CaO, Snis et al. obtained a barrier (48 kcal/mol) substantially higher than experiment and argued that temperature-induced vibrations at the surface could contribute to lower the barrier.[9] By distorting the cluster, they were indeed able to find structures that would both increase and reduce the barrier to recombination. For one of these structures, the computed barrier was 25 kcal/mol, which is comparable to the barrier of abstraction. In the present work, we have included the relaxation of the four central ions on the basis of the energy gradients, and we find a substantially lower barrier for the undistorted lattice as reported in Table 3.

TABLE 3: Transition-State Structure (in Å and Degree) and Activation Barrier (kcal/mol) for the Oxygen Recombination Step[a]

substrate	R_1	R_2	R_3	α_1	α_2	$\Delta E^{\#}$
MgO	1.49	2.00	1.92	99.5	45.0	19.6
CaO	1.49	2.19	2.05	92.1	45.7	39.3

[a] See Figure 6 for symbol description.

The barrier to recombination is very sensitive to the lattice parameter and becomes large already for CaO. This trend is continued and we propose, on the basis of our calculations, that the barrier to recombination of surface peroxide ions becomes prohibitive for SrO and BaO. This is mainly due to the long distance separating the anions on these surfaces that forces the internal bond in the peroxide ions on SrO and BaO to be completely broken before the O_2 molecular bond can begin to form. Here, one must instead assume more complex alternative processes involving BaO_2 converting to BaO with the assistance of diffusion of lattice anions and elimination of O_2. Such processes are, however, beyond the scope of the present type of computational models.

To generate the required neighboring peroxide ions at the surface, one can consider two possible mechanisms: (1) surface diffusion of the peroxide ions at low coverage and (2) a high coverage of peroxide ions due to the decomposition of N_2O. The barrier of surface diffusion will be dependent on the lattice parameter in the same way as for the recombination process. For MgO, but not for the remaining oxides, it is thus possible to regenerate the surface through surface diffusion followed by recombination, while having the abstraction from N_2O as the rate-limiting step.

For CaO, the barrier to diffusion has been estimated from earlier model cluster studies at the externally contracted CI level to be 66 kcal/mol.[34] From this result, there can be no oxygen diffusion over the surface at the relevant temperatures and the remaining path to obtain two peroxide ions in adjacent sites prepared for recombination is through deposition of oxygen. The recombination will thus most likely occur at high coverage of peroxide ions on CaO(100). This is consistent with the results of time-resolved reaction studies, which find simultaneous evolution of O_2 and N_2 when N_2O is passed over MgO[35] but a delay in the oxygen evolution for the same reaction over CaO.[3] The computed barrier to the recombination of 39.3 kcal/mol is about 8 kcal/mol lower than that found earlier by Snis and Panas,[9] which we ascribe to the larger, more flexible model used in the present work. The obtained value is still substantially higher than the 31 kcal/mol that was obtained for the regeneration step by Nakamura et al.[3] In the work by Snis and Panas, however, the repulsion between adjacent peroxide ions at the surface was computed to be 2.5 kcal/mol. At full coverage, the two oxygens that recombine would be surrounded by six surface peroxide ions. Likely, the destabilization is approximately additive and one can thus expect a substantially reduced barrier simply through the effect of the high coverage. Thus, we propose that the regeneration of the surface CaO(100) occurs through oxygen recombination but only at high coverage when the peroxide ions have become sufficiently destabilized. For SrO and BaO, the much larger lattice parameter strongly limits the destabilizing interaction between the adsorbates and even the high-coverage situation is insufficient to allow the LH mechanism to be important.

The Elay−Rideal Mechanism. For SrO and BaO, we must consider an alternative process to regenerate the surface, which would operate in the high-surface peroxide-coverage regime and would still be first order in N_2O. An alternative and possible route is the direct reaction between N_2O and a surface peroxide ion according to reaction 3. In the discussion, we will also include MgO and CaO to discuss the relative importance of the LH and ER mechanisms for these cases. For the Mg_9O_9 cluster model, the adsorbate in the transition state interacts directly with the lattice ions that are described using the AIMP approach. To avoid this, a larger cluster model ($Mg_{10}O_{10}$) was used (see Figure 8). For CaO, SrO, and BaO, the lattice parameters are larger and we did not observe any direct interaction between the adsorbate and the AIMP positions in the lattice when using the Me_9O_9 cluster model.

The thermodynamics of this reaction leading to gas-phase species and the regenerated surface is determined by the stabilization of the surface peroxide ions; thus, one would expect a reduced reactivity when going from MgO to BaO, which is the case. The calculated reaction energies show an exothermic reaction for MgO (−41.9 kcal/mol) and CaO (−14.2 kcal/mol) and thermoneutral for SrO (−3.1 kcal/mol) and BaO (4.8 kcal/mol). In contrast to MgO, CaO, and SrO, the formed singlet O_2 ($[O-O_2]^{2-}$ surface complex) remains adsorbed on the BaO surface (the singlet spin state follows from the reaction between singlet N_2O with the closed-shell surface peroxide ion). Including the binding energy (8.6 kcal/mol) of the O_2 to the surface in the energy balance leads to all reactions being exothermic or thermoneutral. On the MgO and CaO (100) surfaces, the O_2 is unstable toward desorption, while for SrO the O_2 adsorption is thermoneutral (1.1 kcal/mol). These results are valid only at low coverage.

The barrier to the ER reaction could again be expected to follow the trends given by the lattice parameters, but since the reacting peroxide ions are stabilized as we go from MgO to BaO, the barrier should increase along this sequence. The reverse trend compared to the abstraction to give the peroxide ions would thus be expected to prevail. The computed barriers in Table 4, however, do not conform to this expectation and instead show a decreasing trend. MgO has the highest barrier (34.8 kcal/mol) to this reaction and BaO has the lowest (20.6 kcal/mol). To understand the origin of this discrepancy, we must consider the detailed structure (see Figure 7) of the transition state. Coordination of the adsorbate toward both the surface oxygen and the cation was investigated and the lowest energy pathway is reported here.

TABLE 4: Transition-State Structures (Å and Degrees) and Activation Barriers (kcal/mol) for the Regeneration Step at the Low-Coverage Limit in the N_2O Decomposition Reaction[a]

subsrate	*R*1	*R*2	*R*3	*R*4	α(NNO)	α(NOO)	α(OOO)	qN_2O	$\Delta E^{\#}$
MgO	1.12	1.61	1.86	1.49	153.7	171.8	98.2	−0.19	34.8
CaO	1.13	1.56	1.90	1.48	152.2	172.9	100.8	−0.25	31.2
SrO	1.13	1.61	1.95	1.48	149.3	174.9	104.5	−0.44	25.9
BaO	1.14	1.71	2.00	1.49	143.1	167.8	103.1	−0.63	20.6

[a] Mulliken total charge on N_2O in the TS is given as qN_2O. Structural parameters are defined in Figure 7.

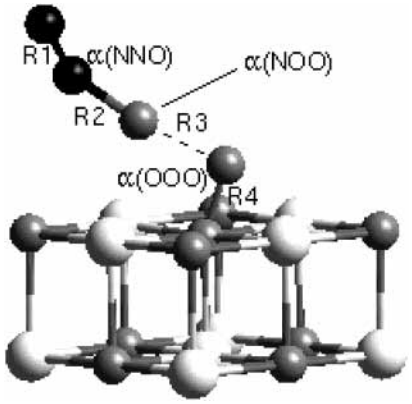

Figure 7. Transition-state structure of the ER surface regeneration step for alkaline-earth oxides at low peroxide ion coverage. See Table 4 for the corresponding geometry data. Oxygen is given in gray, nitrogen in black, and metal in white.

There are several interesting aspects with this transition-state structure. The oxide surface seems here to play a more direct role in the activation process. The transition states for CaO, SrO, and BaO are found for a configuration where there is a favorable electrostatic interaction with the substrate. The internal charge distribution in the N_2O at the TS is negative oxygen, somewhat positive nitrogen bound to the oxygen, and negative outer nitrogen. This is stabilized with the positive nitrogen moving down toward the next surface oxygen anion. The stabilization is highest for BaO, which has the largest lattice parameter and gives the best fit of the TS structure to the underlying lattice. This trend thus counteracts and reverses the expected reactivities. Moreover, the population analysis shows an increased charge donation from the surface to N_2O along the series MgO to BaO (see Table 4). This increased charge donation is reflected in the elongation of the N−O bond distances in the series CaO to BaO. MgO does not follow this trend, at least for the N−O bond distance. In contrast to the other oxides, the N_2O adsorbate in the TS orients itself more toward the cation (see Figure 8). Because of the relatively small lattice parameter of MgO, the oxygen in N_2O moves toward the surface cation, whereas for CaO, SrO, and BaO, the larger

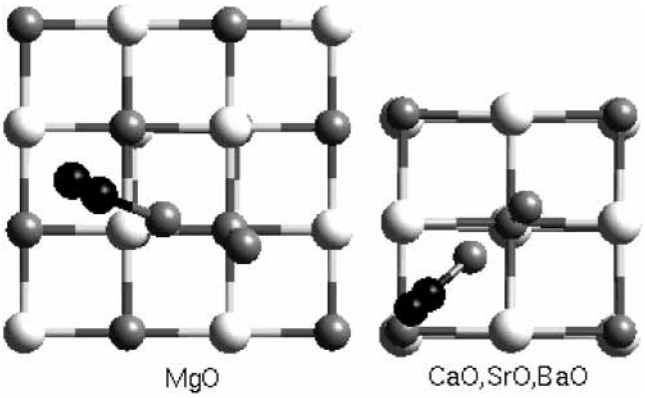

Figure 8. Orientation of N_2O in the ER transition-state structure on the MgO, CaO, SrO, and BaO (100) surface. Oxygen is given in gray, nitrogen in black, and metal in white.

lattice parameters make it more favorable for the positively charged nitrogen to be oriented toward the surface oxygen anion. TS state determination has also been done for the $Mg_{16}O_{16}$ bare cluster. The calculated geometry reveals the same N_2O orientation on the surface as for the embedded case. Moreover, both the calculated activation barrier (36.2 kcal/mol) and the internal geometry are also similar (*R*1: 1. 12, *R*2: 1.62, *R*3: 1.85, *R*4: 1.49, α(NNO): 152.5, α(NOO): 171.1, α(OOO): 98.7) to the embedded case. The vibration frequency analysis shows one imaginary frequency mode (686 cm^{-1}) which corresponds to the mode that transfers the oxygen in N_2O to surface peroxide.

The computed barrier for the BaO surface regeneration reaction according to the low-coverage ER mechanism is 20.6 kcal/mol, which still is substantially lower than the experiment. However, this barrier is higher than the barrier for the direct abstraction with a surface anion, so this pathway should not open up until at higher coverage where it will be difficult to find free surface anion sites to react with. The higher coverage of surface peroxide ions would, however, also result in the elimination of the favorable electrostatic interaction with the surface in the ER transition state found for the low-coverage situation discussed above.

We have for BaO considered the effect of surface peroxide ion coverage on the surface regeneration reaction.[36] We find that the ER barrier is increased through the presence of neighboring peroxide ions and at full coverage the barrier has become 34.3 kcal/mol. This is within the error bars of 33 kcal/mol determined by Xie and Lunsford[16] and also explains the inhibitory effect of O_2 on the decomposition reaction since a surface layer of peroxide ions is observed upon exposure.

In the present work, we have applied an ideal model where we have a stoichiometric BaO compound. In previous experimental works, the picture is more complicated, and nonstoichiometric compounds should be considered. In contrast to what is found for MgO and CaO, surface peroxide ions can be formed from O_2 on BaO. Previous work on alkaline-earth oxides shows that only BaO_2 and SrO_2 are thermodynamically stable, while CaO_2 and MgO_2 are only stable as samples containing water or hydrogen peroxide (see work by Koeningstein and Catlow[37]). During the course of the reaction with N_2O, surface peroxide ions, bulk peroxide ions, and crystalline BaO_2 are most likely formed.

It seems that the mechanism for N_2O decomposition depends on the actual structure and composition of the BaO material. In the work by Xie and Lunsford,[16] the N_2O decomposition already started at 300 °C but did not approach full conversion before 750 °C. The high temperature is needed to regenerate the surface. Xie and Lunsford ascribe this high temperature to the poisoning effect of the formed peroxide ions, which is in agreement with the proposed higher-barrier ER mechanism in the present work.

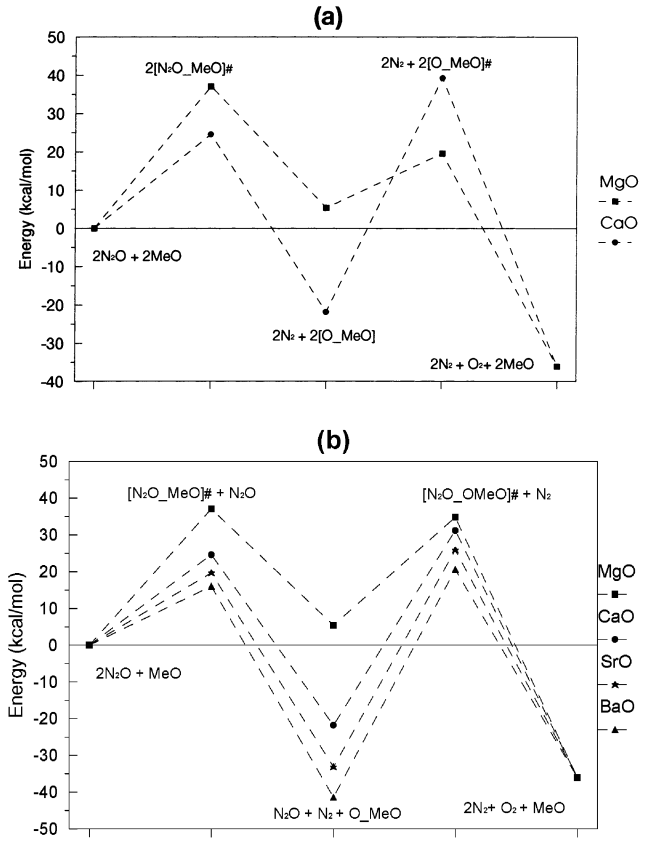

Figure 9. Reaction profiles of the N_2O decomposition reaction for the various substrates. Figure a shows the LH mechanism for the regeneration step. Here, the reaction profile describes decomposition over two independent active sites. In figure b, the reaction profile is displayed for the regeneration of the surface through the ER mechanism.

4. Summary and Conclusion

We can summarize the expected steps (see Figure 9) in the cycle to decompose N_2O on regular terrace sites as follows for the different substrates. For MgO, the binding energy of surface peroxide ions (37.3 kcal/mol for the $Mg_{25}O_{25}$ gas-phase cluster) suggests that the oxygen abstraction step is close to thermoneutral for a five-coordinated oxygen site. The activation barriers for the oxygen recombination step (19.6 kcal/mol at low-peroxide coverage) and the ER surface regeneration step (34.8 kcal/mol) are both lower than the activation barrier for the oxygen abstraction step (37.1 kcal/mol), which could make the oxygen abstraction the rate-determining step in the N_2O decomposition reaction; this will also depend on the preexponential factor, however. The surface is regenerated through oxygen recombination already at low coverage of peroxide ions because of surface oxygen diffusion.

For CaO, the higher stability of the peroxide ions leads to a lower barrier for the oxygen abstraction step. The calculated diffusion barrier suggests that diffusion of surface oxygen over the surface is unlikely.[34] The recombination instead occurs as a result of higher coverage of peroxide ion obtained through the N_2O decomposition. The LH mechanism barrier is here most probably reduced with higher coverage whereas the ER mechanism barrier is increased. Neither should start until high

coverage has been reached since the barrier to the initial oxygen abstraction is much lower. This is in agreement with the analysis of the kinetics presented in ref 13. In the present work, the activation barrier for the LH mechanism at low coverage is calculated to 39.3 kcal/mol. The experimentally determined value is 31 kcal/mol. The destabilization of a peroxide ion because of the presence of a second peroxide ion in a neighboring site has been estimated to be 2.5 kcal/mol.[9] At full coverage, the two recombining peroxide ions would be surrounded by an additional six peroxide ions and it seems likely that this would bring the computed barrier for this step down toward the experimental value. For the ER mechanism, the activation barrier at low coverage is determined to be 31 kcal/mol, but this will increase at higher coverage as the stabilization of the transition state from surface anions is decreased by deposition of oxygen. Thus, the surface regeneration will occur through the LH mechanism. It does not seem necessary to introduce thermal vibrations, as suggested in ref 9 to understand the barrier to recombination.

SrO and BaO have the highest stability of the peroxide ions and consequently the lowest barriers to the decomposition reaction involving the surface oxygen anions. We conclude that because of the lattice parameter there is no diffusion of oxygen over the surface and recombination of surface peroxide ions has a prohibitive barrier. The regeneration of the surface occurs through the ER mechanism, which is still first order in N_2O and thus not in disagreement with the work of Xie and Lunsford.[16] O_2 remains bound to the surface for BaO at low coverage with a computed binding energy of 8.6 kcal/mol. This is most likely reduced at full coverage and O_2 is not expected to bind to the peroxide-covered surface. The high barrier found for the ER mechanism at high-peroxide coverage could explain the inhibitory effect of O_2 on the decomposition reaction

SrO forms an interesting intermediate case with about similar and reasonably low barriers for the two steps. In this case, the abstraction and regeneration steps would run approximately equally efficiently at the same temperature and this would be an interesting case for experimental study.

Acknowledgment. All the calculations were performed on Origin2800/3000 located at NTNU in Trondheim. The computer facility at NTNU is organized under the NOTUR program. We thank the staff at NTNU for the technical support.

References and Notes

(1) Environmental Signals 2001; Environmental assessment report no. 8; OPOCE, EEA: Copenhagen, Denmark, 2001.
(2) Kapteijn, A.; Rodriguez-Mirasol, J.; Moulijn, J. A. *Appl. Catal., B* **1996**, *9*, 25.
(3) Nakamura, M.; Mitsuhashi, H.; Takezawa, N. *J. Cat.* **1992**, *138*, 686.
(4) Pacchioni, G.; Ricart, J.; Illas, F. *J. Am. Chem. Soc.* **1994**, *116*, 10152.
(5) Nygren, M.; Pettersson, L. G. M. *Chem. Phys. Lett*. **1994**, *230*, 456.
(6) Horino, H.; Liu, S. W.; Hiratuka, A.; Ohno, Y. *Chem. Phys. Lett*. **2001**, *341*, 419.
(7) Yoshizawa, K.; Yumura T.; Shiota Y.; Yamabe, T. B. *Chem. Soc. Jpn*. **2000**, *73*, 29.
(8) Chiesa, M.; Giamello, E.; Murphy, D. M.; Pacchioni G.; Paginini, M. C. *J. Phys. Chem. B* **2001**, *105*, 497.
(9) Snis, A.; Panas I. *J. Chem. Phys*. **1995**, *103*, 7626.
(10) Schneider W. F.; Hass, K. C.; Ramprasad R.; Adams, J. B. *J. Phys. Chem. B* **1998**, *102*, 3692.
(11) Schneider, W. F.; Hass, K. C.; Rambrasad, R.; Adams, J. B. *J. Phys. Chem. B* **1997**, *101*, 4353.
(12) Triguero, L.; deCarolis, S.; Baudin, M.; Wojcik, M.; Hermansson, K.; Nygren, M.; Pettersson, L. G. M. *Faraday Discuss.* **1999**, *114*, 351.
(13) Snis, A.; Miettinen, H. *J. Phys. Chem. B* **1998**, *102*, 2555.
(14) Idriss, H.; Barteau, M. *Adv. Catal.* **2000**, *45*, 261.
(15) Wyckoff, R. W. G. *Crystal Structures*, 2nd ed.; Wiley: New York, 1963; Vol. 1.
(16) Xie, S.; Lunsford, J. *Appl. Catal. A* **1999**, *188*, 137.
(17) Barandiarán Z.; Seijo, L. *J. Chem. Phys*. **1988**, *89*, 5739.
(18) Barandiarán Z.; Seijo, L. In *Computational Chemistry: Structure, Interactions and Reactivity*; Fraga, S., Ed.; Elsevier: Amsterdam, 1992.
(19) Parry, D. E. *Surf. Sci.* **1975**, *49*, 433.
(20) Parry, D. E. *Surf. Sci.* **1976**, *54*, 195.
(21) Pettersson, L. G. M.; Seijo, L.; Nygren, M. A. *ECPAIMP: an integral program for ECP and AIMP calculations*.
(22) Nygren, M. A.; Hall, R. J. *ECPAIMP interface to Gaussian 94/98*; 1999.
(23) *Gaussian 98*, revision A.9; Gaussian Inc.: Pittsburgh, PA, 1998.
(24) Nygren, M.; Pettersson, L. G. M.; Barandiarán Z.; Seijo, L. *J. Chem. Phys*. **1994**, *100*, 2010.
(25) Pascual, J.; Seijo, L.; Barandiarán, Z. *J. Chem. Phys*. **1993**, *98*, 9715.
(26) Pelmenschikov, A. G.; Morosi, G.; Gamba, A.; Coluccia, S. *J. Phys. Chem. B* **1998**, *102*, 2226.
(27) Tatewaki, H.; Huzinaga, S. *J. Comput. Chem*. **1980**, *1*, 205.
(28) Hay, P. J.; Wadt, W. R. *J. Chem. Phys*. **1985**, *82*, 299.
(29) Dunning, T. H., Jr.; Hay, P. J. In *Modern Theoretical Chemistry*; Schaefer, H. F., Ed.; Plenum: New York, 1976; Vol. III, pp 1−28.
(30) Kantorovich, L. N.; Gillan, M. J. *Surf. Sci.* **1997**, *374*, 373.
(31) Lu, X.; Xu, X.; Wang, N.; Zhang, Q. *J. Phys. Chem. B* **1999**, *103*, 3373.
(32) Herzberg, G. *Electronic spectra of polyatomic molecules*; Van Nostrand Reinhold: New York, 1966.
(33) Pacchioni, G.; Ricart, M. J.; Illas, F. *J. Am. Chem. Soc*. **1994**, *116*, 10152−10158.
(34) Strömberg, D. *Surf. Sci*. **1992**, *275*, 473.
(35) Kobayashi, H.; Hara, K. *ACS Symp. Series (Catal. Transient Cond.)* 1982, *178*, 163.
(36) Karlsen, E.; Pettersson L. G. M. *J. Phys. Chem. B*. **2002**, *106*, 5719.
(37) Koeningstein, M.; Catlow, C. R. A. *J. Solid State Chem.* **1998**, *140*, 103.